Bending Collapse of Thin-Walled Multi-Cell Square Tubes

Syarifah Fairuza*[1], Sigit P. Santosa[2], Annisa Jusuf[3], Leonardo Gunawan[4]

{fairuzalattas@yahoo.com[1], sigit.santosa@itb.ac.id[2], annisajusuf@ftmd.itb.ac.id[3], gun@ftmd.ac.id[4]}

Faculty of Aerospace Technology, Air Marshal Suryadarma University[1]
Faculty of Mechanical and Aerospace Engineering, Institute of Technology Bandung[2,3,4]

Abstract. The side impact collision is the second highest fatality in four-wheeled vehicle accidents after the frontal impact collision. Side collision can result in serious injury to both passenger and driver. The vehicle structure that protects passengers from side collisions is B-Pillar structure, this structure will experience bending crush and absorb collision energy. This study aims to understand the bending collapse behavior of the B-Pillar when given an impact load. There are 4 types of platforms analyzed in this study; single-cell, multi-cell, web-cell and flange-cell. Web-cells are cells that are placed vertically on the cross-section of thin-walled beams, while the flange-cells are cells that are placed transversely on the cross-section of the beams. Aluminum alloy 6061-T6 was chosen for its strength and ease of manufacture. In this study, three-point bending modeling will be carried out, considering the value of punch-displacement, moment-rotation, energy absorption, and specific energy absorption using LS-Dyna. The position of the cell placement is very influential in the study of three-point bending. This is proven by web 3 cells and flange 3 cells which have the same mass and number of cells but have different energy absorption, which are 491.1 J/kg for web 3 cells and 618.1 J/kg for flange 3 cells. Of the four types of platforms studied, those with the highest peak force are multi-cell, followed by web-cell, flange-cell and single-cell.

Keywords: Bending collapse, Three-point Bending, Multi-cell, Energy Absorption.

1. Introduction

When a vehicle crashed at its side, this is known as a side impact. In side collisions, there is limited space between the passengers and the side structure of the vehicle affected by the impact, which can cause passengers and drivers to suffer a serious injury. Crashworthiness was introduction as an attempt to reduce injuries and deaths, increase safety and protect driver and passengers when accidents occur. According to Bois et al. [1] Crashworthiness is the ability of vehicle structure to absorb crash energy. The structure affected by a collision will deform plastically and slow down the transfer of crash energy and provide space to limit the passenger's bodily injury during an accident.

AVINER 2023, November 08-09, Jakarta, Indonesia

DOI 10.4108/eai.8-11-2023.2345843

One part of the vehicle that protects passengers from side collisions is the B-Pillar structure as shown in Fig 1. This structure will experience bending crush when hit by an impact. Bending collapse in thin-walled tubes is one of the most important energy dissipation mechanisms in transverse impact loads. However, bending collapse in thin-walled tubes has received less studies compared to longitudinal impact. This might be as a result of the four wheels' front construction, which can absorb a lot more collision energy than the side structure. [2].

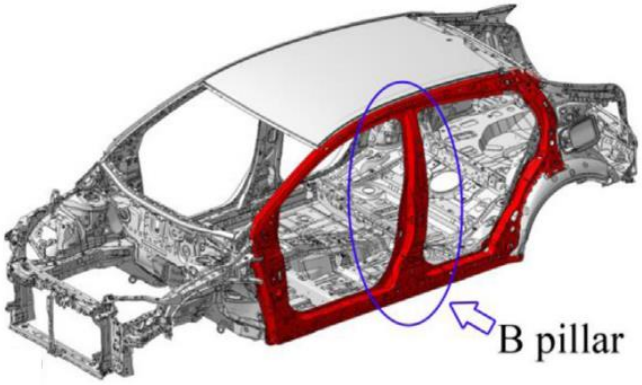

Fig 1. B-Pillar structure [3]

Axial collapse analysis is much simpler than bending collapse analysis since the speed, position, size, and shape of the impactor all have a greater impact on the bending collapse beam response. Wang et al. [2] conducted three-point bending research using partition plates in the longitudinal and cross-sectional directions of the beam to form a multicell structure. They discovered that partition plates had a significant impact on bending resistance, however increasing the number of partitions did not always absorb more energy. Then Huang and Zhang [4] also conducted three-point bending study on thin-walled beams and discovered that span, cross-sectional geometry, and impactor diameter also had significant impact on bending collapse. Zhang et al. [5] conducted research on three-point bending with thickness variations of the web and flange of thin-walled beams. Their optimization results show that a thin flange and a thick web are the best configuration way to increase the bending resistance under transverse loading.

This study will conduct three-point bending collapse of thin-walled beam with variation of beam's cross-section by considering punch force-displacement, moment-rotation, energy absorption (EA), and specific energy absorption (SEA). Energy absorption is defined as the energy absorbed during an impact. Through the deformation of the thin-walled beam structure, kinetic energy is converted into internal energy throughout this energy absorption process. Energy absorption can be obtained by integrating crushing force with structural displacement. Where F is force, and d is displacement of the beam.

$$EA = \int_{d}^{0} F(x)dx \quad (1)$$

Specific energy absorption is a criterion for measuring the energy absorption capacity of thin-walled beam structures. This criterion is defined by the ratio of the total absorption energy (EA) to the mass (m) of the thin-walled beam.

$$SEA = \frac{Etotal}{m} \quad (2)$$

2. Experiment

The three-point bending test was carried out on thin-walled beams using the Instron quasi-static compression test equipment Fig 2. with a speed of 0.5 mm/s, at the FTMD-ITB Light Structures Laboratory. This experimental analysis was carried out in order to validate the numerical analysis with the same geometry, material and setup. The test was conducted using a square specimen of 45 x 45 x 1.5 mm, 470 mm in length, 370 mm in span, and an impactor with a cylindric shape measuring 25 mm in diameter and 100 mm in length.

Fig 3. shows the deformation that occurs in a) single-cell thin-walled beams and b) 2x2 multi-cell. In this figure the thin-walled beam is distorted by the impactor's quasi-static movement before it strikes the top surface of the beam, forming a bending collapse mode. The deformation of a) single cell shaped as an out-ward fold web which occurs from the top flange to the bottom flange. Meanwhile, in the b) multi-cell 2x2 deformation, an out-ward fold web is formed from the top flange surface to the center flange cell. This occurs because the flange-cell prevents the web-cell from forming an out-ward fold web. This type of deformation occurs both in the numerical and experimental test. This proves that the simulated phenomena correspond the actual phenomena conducted by experimental test.

Fig 4 shows a comparison of punch force-displacement resulting from numerical and experimental methods. The trend line experienced by the two methods is comparable, as can be seen from the curve. The quasi-static assumption can be realized, If the proportion of kinetic energy to internal energy is less than 5%, allowing for the control and disregard of inertial effects. Fig 5. shows the internal energy and kinetic energy curves in the quasi-static simulation. The ratio between kinetic energy and internal energy on this curve is 0.3%. It can be seen that the kinetic energy can be neglected because it has a very small value compared to the internal energy, this proves the quasi-static behavior in numerical simulations.

Fig 2. Quasi-static compression testing machine

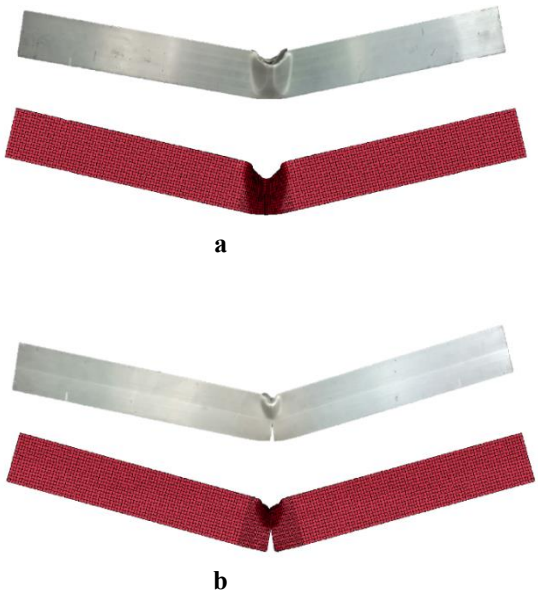

Fig 3. Experiment and Numeric deformation pattern a) *Single-Cell* b) *Multi-Cell 2x2*

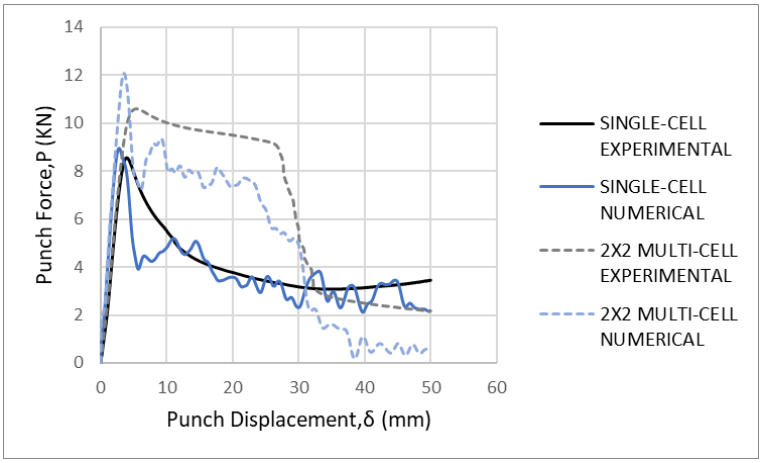

Fig 4. *Punch force-displacement Curve*

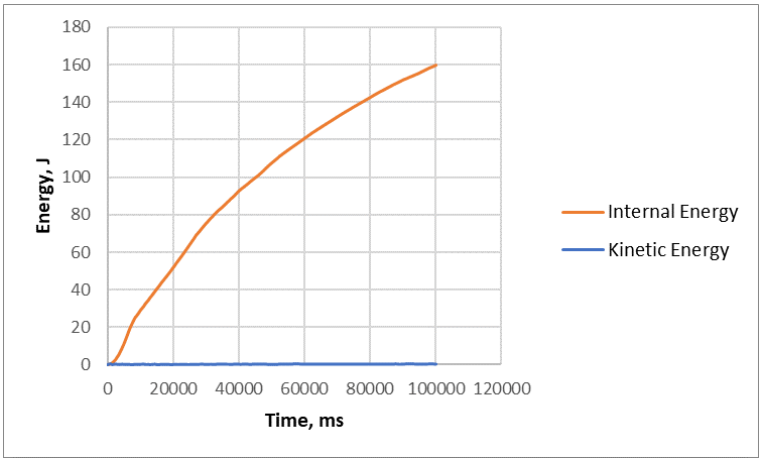

Fig 5. Internal and kinetic energy curve

3. Modeling

For thin-walled beams, the material used is AA6061-T6. AA 6061-T6 material data was obtained from the default data in the Hyperxtrude software. Table 1. contains the material properties of AA 6061-T6. The material properties for the impactor are as follows, E = 193 GPa and $\rho = 0.001036$ kg/m^3 so the mass of the impactor is equal to 50 kg. Impactor material is a material that is modeled on the initial basis of the mass to be obtained.

Table1. Material property

Property	Symbol	Value	Units
Density	ρ	2.7e-06	Kg.mm^{-3}
Yield Strength	σ_y	0.271	GPa
Young's Modulus	E	69.28	GPa
Possion's Ratio	υ	0.35	-

Fig 6. shows the geometry that will be used in the three-point bending simulation, in the form of a thin-walled square beam with dimensions of 45 x 45 x 1.5 mm, a cylindrical impactor and support with a diameter of 25 mm, a length of 100 mm and a mass of 50 kg. Fig 7 shows variations in the cross-section of thin-walled beams which will be simulated with three-point bending loading. Cross-section variations consist of single-cell, web-cell, flange-cell, and multi-cell cross-sections. Web-cell is a cell that is formed by placing a partition vertically on the cross-section of the beam, flange-cell is a cell that is formed by

placing a partition transversely on the cross-section of the beam, and multi-cell is a cell that is a combination of web-cell and flange-cell. which have the same number of cells.

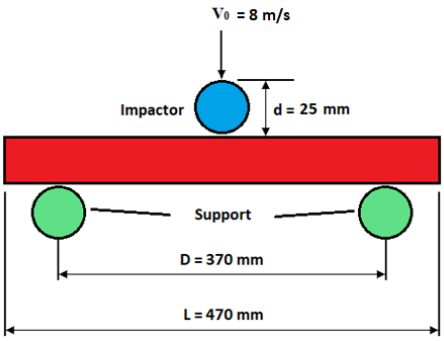

Fig 6. Geometry and dimension for three-point bending test

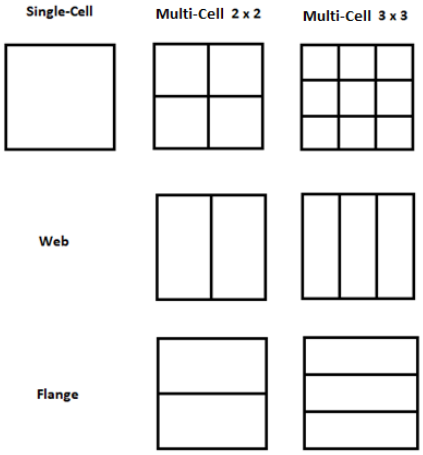

Fig 7. Specimen cross-section variation

The three-point bending model in this study consists of an impactor with falling speed of 8 m/s, a thin-walled beam with varying cross-sections and two supports as in Fig 8. The impactor and support are cylindrical with a diameter of 25 mm and a length 100mm. Thin-walled beams 470 mm long are placed on supports with a span of 370 mm.

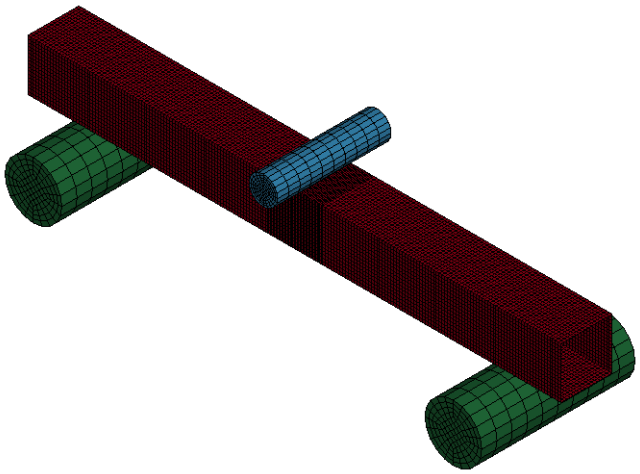

Fig 8. Three-point bending model before impact

Thin-walled square beams are modeled using Mat 107 Modified Johnson-Cook constitutive model whose phenomena are formulated in Equation 3, where σ_{eq} is equivalent stress, ε_{eq} is equivalent plastic strain and *A, B, n, C* and *m* are material properties.

$$\sigma_{eq} = (A + B\varepsilon_{eq}{}^{n})(1 + \dot{\varepsilon}_{eq}{}^{*})^{C}(1 - T^{*m}) \quad (3)$$

The failure model for thin-walled beams uses the Cockcroft-Latham fracture criterion which is part of the Mat 107 model. This criterion is written in Equation 4, where W is the plastic work per unit volume, W_{cr} is the critical parameter determined based on uniaxial tensile testing, σ_1 is the major principal stress, $(\sigma_1) = \sigma_1$ while $\sigma_1 \geq 0$ and $(\sigma_1) = 0$ while $\sigma_1 < 0$.

$$W = \int_0^{\varepsilon_{eq}} (\sigma_1) d\varepsilon_{eq} \leq W_{cr} \quad (4)$$

Table 2. Mat-107 Modified Johnson-Cook Parameter

Yield stress, A	0.260	*(GPa)*
Hardening parameter, B	0.123	*(GPa)*
Hardening parameter, n	0.288	-
Strain rate sensitivity, C	0.001	-
Reference strain rate, ε_0	0.001	*(s^{-1})*
Critical Cockcroft-Latham parameter, W_{cr}	0.535	*(GPa)*

4. Result

4.1 Web-Cell Effect

Fig 9. shows the deformation that occurs in single-cell and web-cell is bending collapse mode deformation, where the bending is concentrated at the top flange cell of the beam. The inward bend at the impactor's fall position forms an out-ward fold web which is formed from the top flange cell to the bottom flange cell. During web-cell deformation, no cracks were found at the bottom of the cell. Fig 10. shows the punch force-displacement curve from the numerical simulation results of three-point bending on beams with single-cell and web-cell cross-sections. From this curve, it can be seen that the trend lines experienced by the following two cross-sectional are not much different, after the occurrence of the maximum peak followed by the upward and downward curves with an increasingly diminishing amplitude.

Fig 9. Deformation pattern of single-cell and web-cell

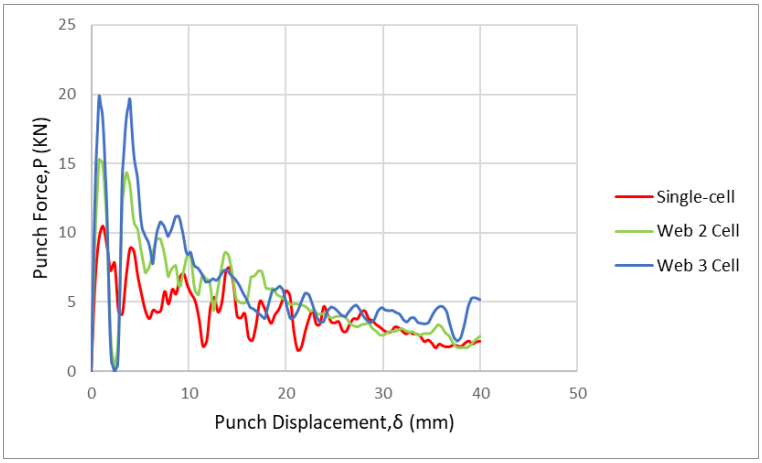

Fig 10. *Punch-force displacement web-cell*

Table 3. are the results of three-point bending numerical simulations on single-cell and multi-cell cross-sections with impactor distance of 40 mm. Judging from the total mass, peak force, ultimate bending moment, and energy absorption, all of these parameters rises with the increase of the cells. Sorted from smallest are single-cell, 2-cell web and 3-cell web. However, if you look at the specific energy absorption, 2-cell web is the highest, followed by the 3-cell and single-cell web. From these data, it can be concluded that adding web-cells to the cross-section of the beam in three-point bending loading can increase specific energy absorption but had to consider the total mass of the beam, since the mass of the beam is increasing as well as the specific energy absorption, see Equation 2.

Table 3. Simulation results of web-cell cross-sections

Cross Section	*Thin-walled Mass (kg)*	*Peak Force (kN)*	*Ultimate Bending Moment (Nm)*	*Critical Bending Rotation (degree)*	*Energy Absorption (J)*	*SEA (J/kg)*
Single-cell	0.342	10.5	1231.2	0.29	163.3	477.4
Web 2 Cell	0.428	15.3	1798.2	0.19	213.2	498.1
Web 3 Cell	0.513	19.8	2330.8	0.19	252.0	491.1

Table 4. Web-cell differences

Cross Section	*Peak Force (kN)*	*Difference (%)*	*SEA (J/kg)*	*Difference (%)*
Single-Cell	10.5	-	477.4	-
Web 2 Cell	15.3	46.1	498.1	4.3
Web 3 Cell	19.8	89.3	491.1	2.9

Table 4 provides information regarding the differences of peak force and SEA for single-cell and web-cell cross-sections. Peak force rise as the number of web-cells increase, this is proven by the value of peak force increase by 29.4% difference. But not for the value of SEA, which decreasing by 1.4%. This decrease caused by the mass of the beam which is also included in the SEA calculation.

4.2 Flange-Cell Effect

Flange-cell is a cell that is formed due to the placement of a partition in the transverse direction of the beam cross-section. Fig 11. shows the form of deformation that occurs in single-cell and flange-cell cross-sections. The deformation that occurs in the flange-cell configuration is a bending collapse mode deformation that is accompanied by indentation, where the bending concentrated at the top of the beam flange cell. This deformation also consists of Inward bending and out-ward fold web which the forming of this out-ward fold and a crack also occurs at the bottom of the cell, this is because the flange-cell inhibits the bending process in the beam.

Fig 11. Deformation pattern of single-cell and flange-cell

Fig 12 shows the punch force-displacement curve from the numerical simulation results of three-point bending on beams with single-cell and flange-cell cross-sections. From this curve, it can be seen that the trend lines experienced by the following two cross-sectional variations have slight differences. In the cross-section of the flange 2 cell and the flange 3 cell, the maximum peak occurs at the third peak of the curve, which is slightly higher than the first peak. This is because the beam has undergone plastic deformation before the rebound occurs, the first peak is the result of the indentation, and the third peak is the result of bending process.

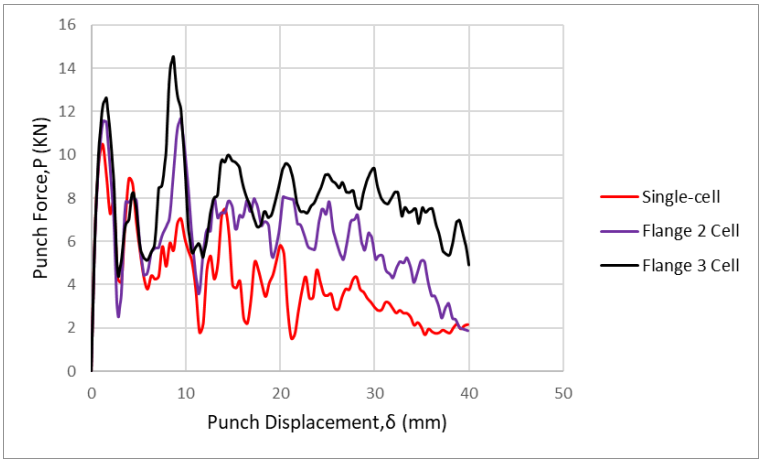

Fig 12. *Punch-force displacement flange-cell*

Table 5. Simulation results of flange-cell cross-sections

Cross Section	*Thin-walled Mass (kg)*	*Peak Force (kN)*	*Ultimate Bending Moment (Nm)*	*Critical Bending Rotation (degree)*	*Energy Absorption (J)*	*SEA (J/kg)*
Single-cell	0.342	10.5	1231.2	0.29	163.3	477.4
Flange 2 Cell	0.428	11.7	1373.7	2.32	246.3	575.6
Flange 3 Cell	0.513	14.5	1707.3	2.12	317.1	618.1

Table 5. is the results of numerical simulations of three-point bending on single-cell and flange-cell cross-sections which have been calculated at an impactor distance of 40 mm. considered from the value of total mass, peak force, ultimate bending moment, energy absorption and specific energy absorption, all of these parameters increase with the increase in the number of cells, sorted from smallest are single-cell, 2-cell flange and follow with the 3-cell flange.

Table 6. *Flange-cell differences*

Cross Section	*Peak Force (kN)*	*Difference (%)*	*SEA (J/kg)*	*Difference (%)*
Single-Cell	10.5	-	477.4	-
Flange 2 Cell	11.7	11.6	575.6	20.6
Flange 3 Cell	14.5	38.7	618.1	29.5

Table 6. provides information regarding the differences of peak force and SEA for single-cell and flange-cell cross-sections. Peak force and SEA values increase with the presence of the flange-cells, this proven by the rise of peak force by 23.9% and rise of SEA by 7.3% along with the increase in the number of flange-cells in the beam.

4.3 Multi-Cell Effect

Multi-cell is a combination of web-cell and flange-cell which had the same number of cell. The deformation that occurs in multi-cells is bending collapse mode deformation where the bending is concentrated at the top cell of the beam. This form of deformation is the same as the form of deformation that occurs in web-cell deformation. Additionally, there is an outward fold web formed by an inward bend where the impactor hits, which is followed by a crack that originates at the bottom cell and ends at the first flange-cell that the crack first meets, see Fig13.

Fig 14 shows the punch force-displacement curve from the numerical simulation results of three-point bending on beams with single-cell and multi-cell cross-sections. From this curve, it can be seen that the trend lines experienced by the following two cross-sectional variations are not much different, instead they are at different amplitude.
In Table 7, the critical bending rotation that occurs in multi-cell 2x2 and multi-cell 3x3 is the same, at 0.27^0. And the critical bending rotation that occurs in multi-cells has slightly lower than single-cells. Except the critical bending rotation, the value of all properties increasing as the number of multi-cell increase. This is proven by the rise of the peak force by 31.9% and the SEA by 17.7%, see Table 8.

Fig 13. Deformation pattern of single-cell and multi-cell

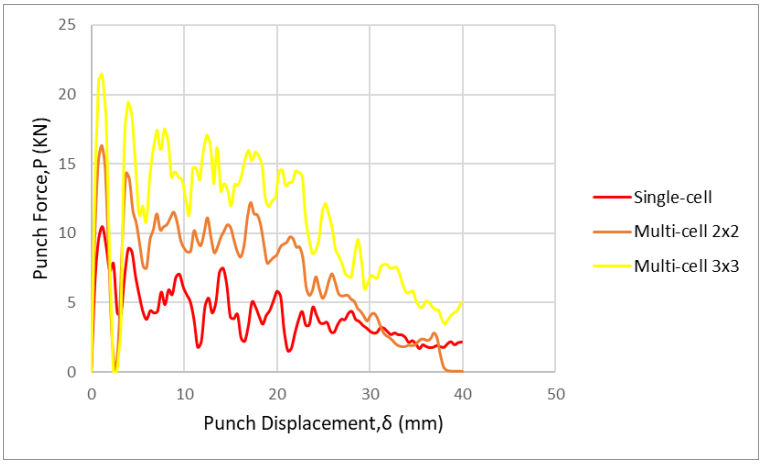

Fig 14. *Punch-force displacement multi-cell*

Table 7. Simulation result of *multi-cell cross-section*

Cross Section	*Thin-walled Mass (kg)*	*Peak Force (kN)*	*Ultimate Bending Moment (Nm)*	*Critical Bending Rotation (degree)*	*Energy Absorption (J)*	*SEA (J/kg)*
Single-cell	0.342	10.5	1231.2	0.29	163.3	477.4
Multi-cell 2x2	0.513	16.3	1918.2	0.27	277.1	540.2
Multi-cell 3x3	0.685	21.5	2521.6	0.27	435.6	635.9

Table 8. *Multi-cell differences*

Cross Section	*Peak Force (kN)*	*Difference (%)*	*SEA (J/kg)*	*Difference (%)*
Single-Cell	10.5	-	477.4	-
Multi-Cell 2x2	16.3	55.8	540.2	13.1
Multi-Cell 3X3	21.5	104.8	635.9	33.2

4.4 Cross-section Comparison

Fig 15 shows the deformation that occurs in various cross-sections of thin-walled beams after three-point bending simulation with an initial speed of 8 m/s. The comparison of deformation shapes in this cross-sectional variation is represented by a single-cell cross-section and a cross-section with a total of 3 cells. It can be seen in the Figure that all cross-sectional variations have a concentration of bending in the top-cell region of the beam at the location where the impactor falls and forms a bending collapse mode deformation. However, unlike the flange-cell, this section experiences bending collapse deformation with indentation. It can be seen from the deformation of cross section that contain flange cell such as multi-cell and flange-cells cross-sections have cracks at the bottom cell of beam. Having flange-cells can also prevent the formation of out-ward fold web, where the formation stops at the first flange cell that is impacted. In contrast to cross-sections that do not have flange cells such as single-cell and web-cell, this cross-section does not experience cracks at the bottom flange and out-ward fold deformation in the web-cell cross-section continues to propagate until the bottom cell.

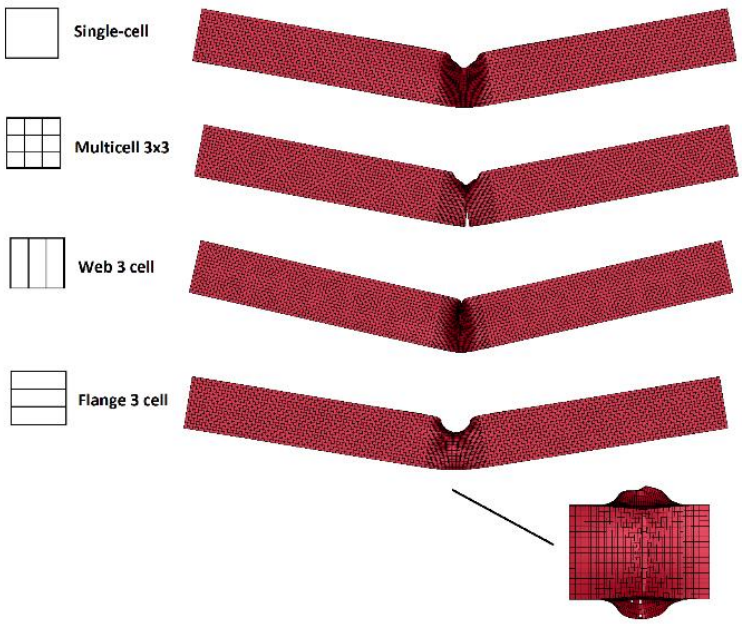

Fig 15. Deformation pattern of cross-section variation

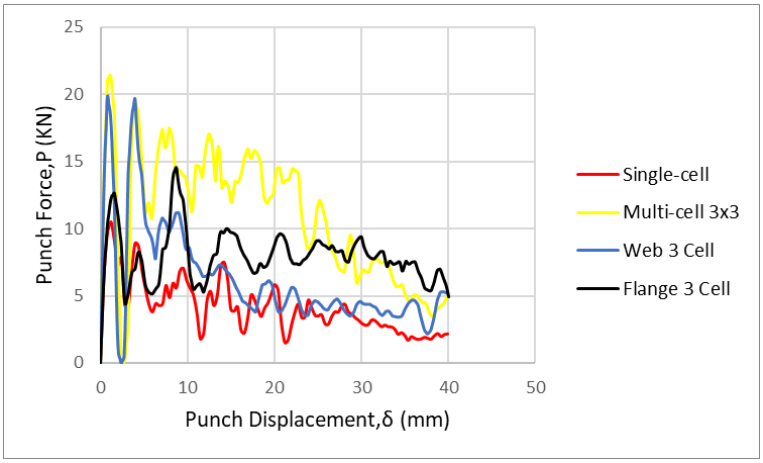

Fig 16. *Punch-force displacement*

Fig 16 shows the punch force-displacement curve from the numerical simulation results of three-point bending carried out at an initial speed of 8 m/s. From these curves it can be seen

that the trend lines experienced by the four variations are not much different. The trend line strat with the maximum peak followed by an up and down curve with decreasing amplitudes. The maximum force peak occurs at the first peak of the curve. However, different from other variations, the flange cell cross-section has a maximum peak that occurs at the third peak of the curve, which is slightly higher than the first force peak. The first peak is the effect due to indentation, the second peak is when an outward fold web is formed which is accompanied by a crack on the bottom flange, while the third peak is the effect of beam bending.

Table 9. Simulation result of cross-section variation

Cross Section	*Thin-walled Mass (kg)*	*Peak Force (kN)*	*Ultimate Bending Moment (Nm)*	*Critical Bending Rotation (degree)*	*Energy Absorption (J)*	*SEA (J/kg)*
Single-cell	0.342	10.5	1231.2	0.29	163.3	477.4
Multi-cell 3x3	0.685	21.5	2521.6	0.27	435.6	635.9
Web 3 Cell	0.513	19.8	2330.8	0.19	252.0	491.1
Flange 3 Cell	0.513	14.5	1707.3	2.12	317.1	618.1

Table 9 shows the results of three-point bending numerical simulations which have been calculated at an impactor distance of 40 mm. considered from the value of peak force and ultimate bending moment, multi-cell 3x3 has the highest value and single-cell has the lowest value of all the four cross-section variations. Then, if we look at the terms of the mass, even though the 3 cell web and the 3 cell flange had the same mass of 0.513 kg and the same number of cells, but they have different value of specific energy absorption as 491.1 J/kg for 3 cell web and 618.1 J/kg for 3 cell flange. This shows that the direction of cell placement in thin-walled beams has a large role in three-point bending studies. Of these four types of platforms, it can be concluded that the one with the highest value of peak force and moment is multi-cell, followed by web-cell, flange-cell, and single cell. However, if we look at the specific energy absorption value, flange-cell has the highest value compared to multi-cell, this is due to the mass of the beam which is also included in the SEA calculation that stated in Equation 2.

5. Conclusion

In this research, three-point bending modeling was carried out, which consists of an impactor with a mass of 50 kg with initial speed 8 m/s, thin-walled beam structure with varying cross-sections, and two supports. By using thin-walled hollow beams, this research aims to understand the bending collapse behavior of the B-Pillar when given impact load. There are 4 types of platforms analyzed, namely single cell, multi cell, web cell, and flange cell. Based on the research, the important point stated as follow:

- Bending collapse mode and bending collapse deformation with indentation, provide different punch force-displacement curve responses. In bending collapse mode, the peak force occurs at the first peak, while in bending collapse with indentation the peak force occurs at the third peak. This is because before the rebound, the beam has undergone plastic changes through the formation of an indent.
- The bending behavior in three-point bending begins with the formation of an inward fold at the impact section, followed by the formation of an outward fold web, followed by bending the beam towards the impact, then ending with a crack at the bottom flange.
- By increasing the number of cells in the cross section, the peak force and ultimate bending moment can increase as well. Of the four types of platforms studied, the one with the highest value of peak force is multi-cell, followed by web-cell, flange-cell, and single-cell.
- The position of cell placement on thin-walled beams has a large role in three-point bending studies. This is proven by the 3 cell web and 3 cell flange which have same total mass and number of cells, but have different specific energy absorption values, namely 491.1 J/kg for 3 cell web and 618.1 J/kg for 3 cell flange.
- Flange 3 Cell is chosen for the best configuration compared with the other platforms. Although its value of SEA is slightly smaller than the multicell 3x3 platform by 2.79% but, its value of peak force is much smaller than the multicell 3x3 platform by 32,55%. These values were taken into consideration because, in order to protect the passenger from the impact collision, the structure of the B-pillar needs to absorb as much energy as possible but with a lesser peak force.

References

1. Bois, P. D., Chou, C. C., Fileta, B. B., Khalil, T. B., King, A. I., Mahmood, H. F., Mertz, H. J. and Wismans, J.: Vehicle Crashworthiness and Occupant Protection, Michigan: *American Iron and Steel Institute* (2004).
2. Wang, Z., Li, Z. and Zhang, X.: Bending resistance of thin-walled multi-cell square tubes, *Thin-Walled Structures*, 107, 287-299 (2016).
3. Dongyong Shi, Kenichi Watanabe, Junya Naito, Kensuke Funada, Kazuya Yasui: Design optimization and application of hot-stamped B pillar with local patchworks blanks, *Thin-Walled Structures*, 170, 108-523 (2022).
4. Huang, Z. and Zhang, X.: Three-point bending collapse of thin-walled rectangular beams, *Int J Mech Sci*, 144, 461-479 (2018).
5. T, Hossein., N, Hassan Moslemi., M, Mohammad Javad., M, Mohammad Ali,. G, Hamid. and A, Sergei.: Ductile fracture prediction of AA6061-T6 in roll forming process, *Mechanic of Material,* vol 148, 103498 (2020).
6. Zhang, X., Zhang, H. and Wang, Z.: Bending collapse of square tubes with variable thickness, Int. J. Mech. Sci, 106, 107–116 (2016).